

USING THERMOMECHANICAL TREATMENTS TO IMPROVE THE GRAIN GROWTH OF NEW-GENERATION ODS ALLOYS

UPORABA TERMOMEHANSKE OBDELAVE ZA IZBOLJŠANJE RASTI ZRN NOVE GENERACIJE ODS ZLITIN

Omid Khalaj¹, Hana Jirková¹, Bohuslav Mašek¹, Parsa Hassasroudsari¹, Tomáš Studecký², Jiří Svoboda³

¹University of West Bohemia, Univerzitní 22, 306 14 Pilsen, Czech Republic

²COMTES FHT a.s., Průmyslová 995, 334 41 Dobřany, Czech Republic

³Institute of Physics of Materials, Academy of Sciences of the Czech Republic, Žižkova 22, 616 62 Brno, Czech Republic
khalaj@vctt.zcu.cz

Prejem rokopisa – received: 2017-12-15; sprejem za objavo – accepted for publication: 2018-02-15

doi:10.17222/mit.2017.148

In order to achieve specific mechanical properties and structures of a material, a combination of new technologies together with an unconventional use of different types of materials could be an asset. Powder metallurgy, involving a metal matrix and dispersed stable particles, in combination with mechanical alloying and hot consolidation could be a solution. This paper describes the thermomechanical characteristics of new oxide-dispersion-strengthened (ODS) alloys with a Fe-Al matrix in terms of changes in the grain-size distribution. Recrystallization and grain growth were investigated over a range of temperatures and deformations. The results show that the grain-growing process in the new ODS alloys is significantly affected by the thermomechanical treatment, leading to the maximum grain size within 20-h annealing at 1200 °C. They are analysed using different methods, including optical microscopy.

Keywords: grain growth, ODS alloys, steel, Fe-Al, Al₂O₃

Da bi lahko izdelali materiale s specifičnimi mehanskimi lastnostmi in strukturo, moramo izbirati kombinacijo več različnih novih tehnologij skupaj z nekonvencionalno uporabo različnih vrst materialov. Kot rešitev se ponuja tehnologija metalurgije prahov, s katero lahko ustvarimo mešanico kovinskih prahov in stabilnih oksidnih delcev. Tej sledi kombinacija mehanskega legiranja in vroče konsolidacije. V članku avtorji opisujejo termomehanske lastnosti nove z oksidi disperzijsko utrjene (ODS; angl: Oxide Dispersion Strengthened) zlitine s Fe-Al matrico s poudarkom na spremembah porazdelitve velikosti kristalnih zrn. Avtorji so raziskovali rekristalizacijo in rast zrn v širokem območju temperatur in deformacij. Rezultati raziskave so pokazali, da je proces rasti zrn novih ODS zlitin pomembno odvisen od termomehanske obdelave, ki vodi do maksimalne velikosti zrn po 20 urnem žarjenju na 1200 °C. Avtorji so za analize uporabili različne metode, vključno z optično mikroskopijo.

Ključne besede: rast zrn, z oksidi disperzijsko utrjene zlitine (ODS), jeklo, Fe-Al, Al₂O₃

1 INTRODUCTION

Historically, oxide-dispersion-strengthened (ODS) alloys have been employed to improve mechanical properties at high temperatures. The first preparation of ODS alloys was reported by W. D. Coolidge in 1910, as a result of using classical powder metallurgy to develop a tungsten-based alloy reinforced with thorium oxides to increase the life span of a tungsten-filament lamp and impede high-temperature grain growth.¹ Continuing this initial development, several other applications based on various metallic matrices such as aluminium or nickel were implemented over the decades. J. S. Benjamin at the International Nickel Company (INCO) laboratory designed a new process based on high-energy milling-powder metallurgy – later called mechanical alloying.² He developed this process to obtain a homogeneous oxide dispersion within a nickel matrix to produce high-temperature-resistant materials for gas-turbine applications.³ Currently, mechanical alloying is still considered to be one of the most effective processes for obtaining fine and homogeneously distributed particles.

In 1829, Félix Savart tried to reproduce the anisotropy effect on various metal specimens to demonstrate that metals consisted of crystallized parts with different orientations.⁴ He also recorded the first signs of a structural change after deformation while treating modified anisotropic properties of metals.⁵ Continuing the improvement in the ODS-alloy microstructure, H. C. Sorby⁶ reported the formation of an equiaxed grain structure during the annealing of elongated grains in deformed iron by introducing a metallographic technique called recrystallization. In the early 1920s, Carpenter and Elam, followed by Altherthum, clearly established that while the grain-boundary energy provides the driving force for grain growth, the stored energy provides the driving force for recrystallization. Deformation is then clearly established as the initiating process for recrystallization. Despite these fundamental discoveries, recrystallization and grain growth had not yet been distinguished as separate processes.

The proportion of dispersed spherical oxides with a mean size of 5–30 nm (typically) in a mixture is usually below 1 %; however, it plays the main role in the stabi-

lity of the microstructure. The resistance to the coarsening of oxides is much higher in coarse-grained ferrite than in the γ' -precipitates in super alloys. Also, for a mean size of 20–30 nm, the limiting temperature for a long-term operation is between 1000 °C and 1100 °C. So, it is clear that oxides are extremely stable and the microstructural stability of ODS alloys is much higher than that of nickel-based super alloys. However, the loss of mechanical properties due to the coarsening of oxides was also reported for fine-grained ODS steels at temperatures of about 800 °C for systems with extremely fine oxide dispersion (about 5 nm).⁷ Thus, it is clear that the size of oxides and the grain size have important roles in the stability of a microstructure. Coarser oxides are much more stable than fine ones, which is in line with the cubic law of coarsening kinetics.^{8–12} The mechanically alloyed powder is then consolidated at high temperatures and pressures to produce bulk material in the form of a bar or tube stock. Subsequently, different thermomechanical treatments are applied to optimize its microstructure and mechanical properties. The processing temperatures are critical during the consolidation step in order to retain the nanocrystalline structure generated during the mechanical alloying and to impede particle coarsening and grain growth.^{13–19}

In the present study, the ODS alloys consist of a ferritic Fe-Al matrix strengthened with about 7 % volume fraction of Al_2O_3 particles. In order to investigate these new groups of materials with a more detailed analysis, this paper concentrates on the mechanical properties of ODS alloys, the microstructure and the phenomenon of recrystallization, leading to an evaluation of the grain growth.

2 EXPERIMENTAL PART

2.1 Material preparation

The method for producing Fe-Al based ODS alloys with fine Al_2O_3 precipitates is highly dependent on powder metallurgy (Figure 1).²⁰ In the first step, the powders consisting of Fe-11 % mass fraction of the Al

matrix (90 % mass fraction of Fe and 10 % mass fraction of Al) are mixed with 1 % mass fraction of O_2 in gas, which is absorbed, in a low-energy ball mill developed by the authors, allowing evacuation and filling by oxygen. It is equipped with two steel containers (each 24 L), filled with 160 (80 in each) steel balls with a diameter of 40 mm. The mill-rotation frequency can be adjusted between 20 min^{-1} to 75 min^{-1} . However, for this study, all the material preparation is done at a constant rate of 75 min^{-1} . After the mechanical alloying, the powder changes to a solid solution and is poured from the milling container into a 70-mm-diameter steel container (made of low-alloy steel), evacuated with a suction pump (degassed) and sealed by welding. Then it is heated to a temperature of 750 °C and rolled in a hot rolling mill to a thickness of 20 mm. In the final step, it is heated again up to a temperature of 900 °C and rolled to a thickness of 8 mm. An approximately 6-mm-thick ODS sheet, covered on both sides with 1-mm-thick scale from the rolling container, is produced in this way. Afterwards, the specimens are cut with a water jet (Figure 2).

In this study, two types of material (Fe-10 % mass fractions of the Al ferritic matrix with different particle sizes and 7 % volume fractions of Al_2O_3) were chosen, as described in Table 1. It should be noted that the oxides (Al_2O_3) were produced with internal oxidation as shown in Figure 1 and were not added manually.

Table 1: Material parameters

Material No.	Material type	Milling time (hours)	Ferritic matrix	Volume % of Al_2O_3	Typical particle size (nm)
1	ODS Alloy	245	Fe10w/%Al	7	20-50
2*	ODS Alloy	245	Fe10w/%Al	7	20-50

* Different rolling force

2.2 Specimen preparation

All the prepared containers were annealed at 1000 °C over 16 h. After normal cooling at room temperature, all

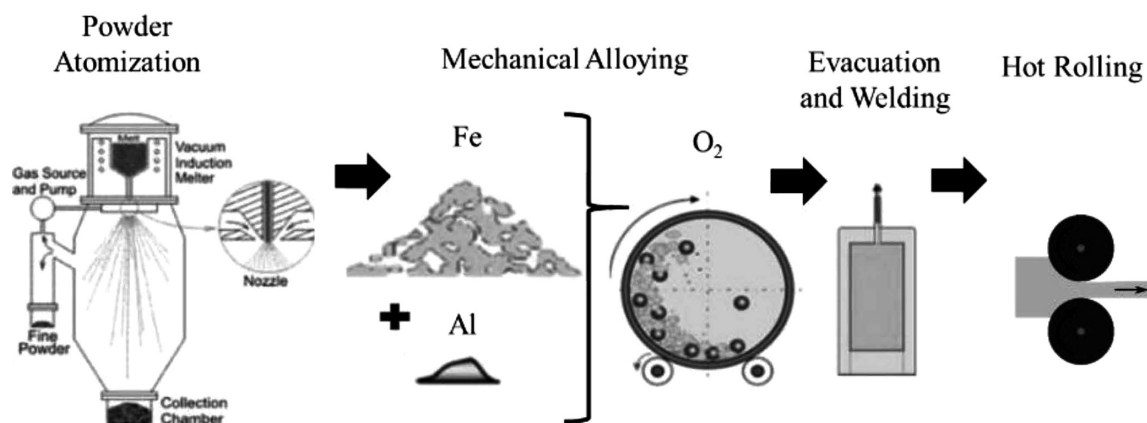


Figure 1: Material-preparation process

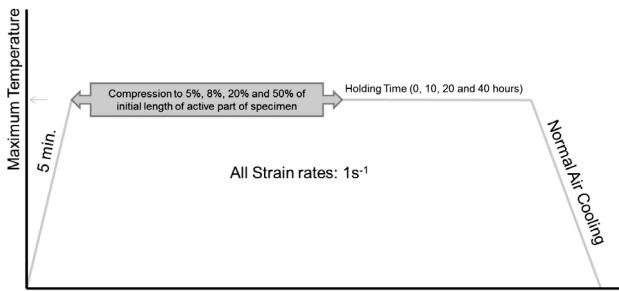


Figure 5: Treatment no. 2

immediately after that the deformation was applied. Subsequently, one specimen of each material was quenched in water for immediate cooling (0-h holding time) and the rest were kept in the furnace for three different holding times of (10, 20, 40) h, after which they were cooled slowly to room temperature.

3 RESULTS AND DISCUSSION

3.1 Test group A

Figure 6 shows the tensile stress-strain curves for both materials at different temperatures corresponding to treatment no. 1.

A comparison of the curves for Material 1 from Figure 6a shows that the modulus of elasticity (E) decreases from 8.6 (RT) to 1.3 GPa (1000 °C) with the increasing

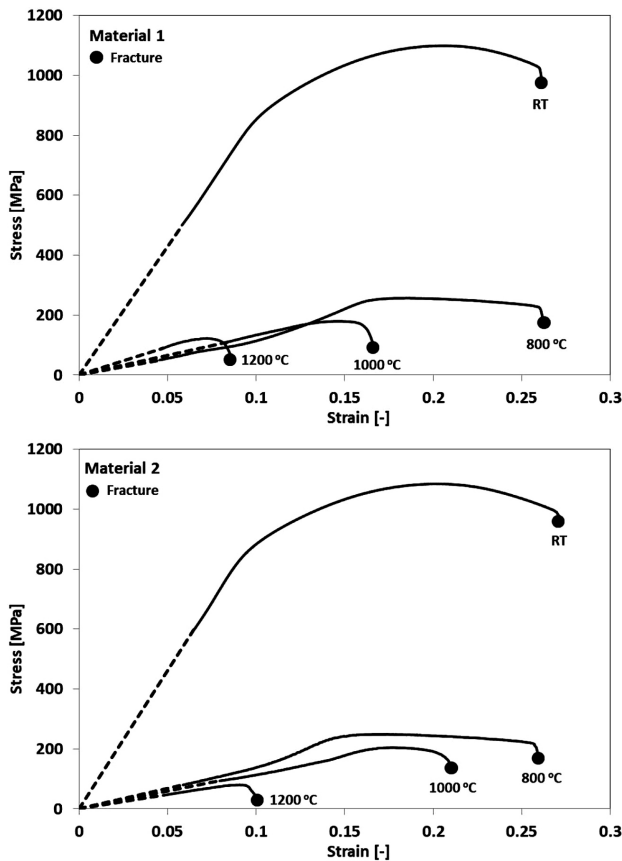


Figure 6: Tensile stress-strain curves for: a) material 1, b) material 2

temperature, to almost 19 % of the initial value at RT. Similarly, the ultimate tensile strength (UTS) decreases from 1100 MPa (RT) to 180 MPa (1000 °C) which shows an almost 86 % reduction from the initial value at RT. Figure 6b shows a similar trend for Material 2. At 1000 °C, the UTS and E decrease by 86 % and 87 %, respectively, in comparison with RT. The work-hardening rate also varies with the temperature, the amount of strain and the composition of the ODS alloy. At lower temperatures, the curve slopes (the modulus of elasticity) are relatively steep from the onset of the plastic deformation to the maximum load. Steep drops in the region between the maximum tensile strength and the fracture point are related to the necking of the specimens.

Table 3 shows the mechanical parameters for both materials from the tensile tests. It can be seen that at the same temperatures, there is a slight difference between the curves of the slopes (E) for each material. It could be that the active energy required for the flow is not simply a function of the applied stress, but rather a complex function involving different factors like the stress, the temperature and the size of the flow units activated by the temperature.

Table 3: Mechanical properties based on the tensile tests

Material no.	Temperature (°C)	E (GPa)	UTS (MPa)	Elongation (%)
1	RT	8.6	1099	14.68
	800	1.1	257	10.80
	1000	1.3	180	8.95
	1200	1.9	122	5.08
2	RT	9.2	1084	16.54
	800	1.4	249	12.45
	1000	1.1	204	7.78
	1200	1.0	80	5.62

It can be seen that the UTS of each material decreases as the test temperature increases. It is almost the same for both materials at RT and 800 °C; however, with further increases in the testing temperature, the difference between both materials increases, which could be attributed to strain aging. Like the UTS , the elongation of both materials increases with the decreasing testing temperature. It is obvious that the total elongation decreases gradually from RT to 800 °C; however, when the temperature is increased to 1200 °C, it jumps to almost 50 % of the initial value at RT for both materials. On the other hand, at higher temperatures, the recovery and damage induced by the creep lead to a decrease in the ductility.^{21–22}

3.2 Test group B

Figure 7 shows the hardness (HV10) test results for both materials without deformation and after the applications of (5, 8, 20 and 50) % deformation, and at different annealing times of (0, 10, 20 and 40) h at 1200 °C. A Vickers hardness test was performed using a ZWICK/

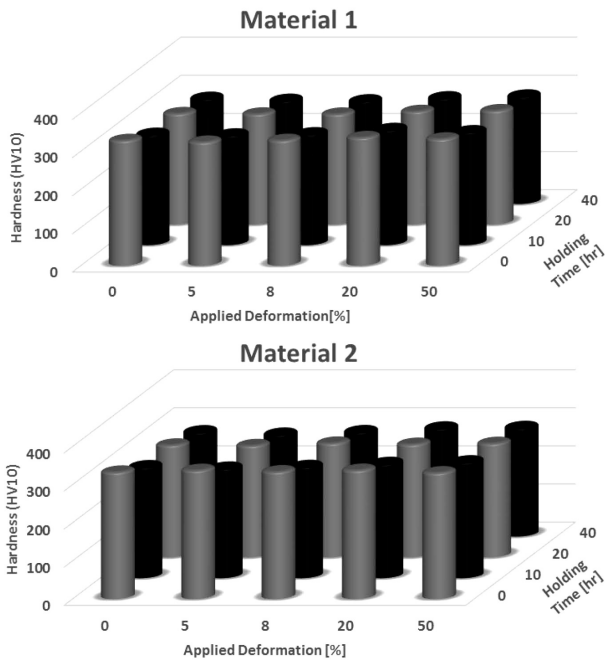


Figure 7: Hardness (HV10) for: a) material 1, b) material 2

ROELL Z2.5 hardness tester with a load of 10 kg and a loading time of 11 s on the surfaces of polished samples. The average value was calculated from three measurements.

It can be seen that with the increasing deformation, there is almost no change in the hardness of either material for any of the holding times. On the other hand, with an increase in the applied deformation from 0 % to 8 %, the hardness decreases slightly at all the annealing times. However, with the increase from 20 % to 50 %, it increases slightly at all the holding times. The hardness values vary from 328 to 332 HV10 (material 1) and 332 to 331 HV10 (Material 2), with no annealing, in the deformation span of 0–50 %. In a similar way, they vary from 277 to 283 HV10 (Material 1) and 274 to 286 HV10 (material 2), for the 40-h holding time at 1200 °C in the deformation span of 0–50 %. It is clear that the decrease in the hardness from 0 % to 8 %, at 1200 °C, is almost 2 %; however, the increase from 8 % to 50 % is maximum, 4 %. It can be generally negligible as the difference between the hardness values is small. However, this small fluctuation can be attributed to the occurrence of a dislocation annihilation or rearrangement followed by a rapid subgrain growth; however, this could be due to the inhomogeneity of the material within the whole container.

Figures 8–15 show the microstructures of both materials without deformation and after 50 % deformation for different annealing times of (0, 10, 20 and 40) h at 1200 °C. The light microscope was used to record the microstructure at the grain and subgrain scale for all the deformations (0, 8, 20 and 50) %; however, due to a large number of images, only those depicting the 0 % and 50 % deformations are presented. The structure con-

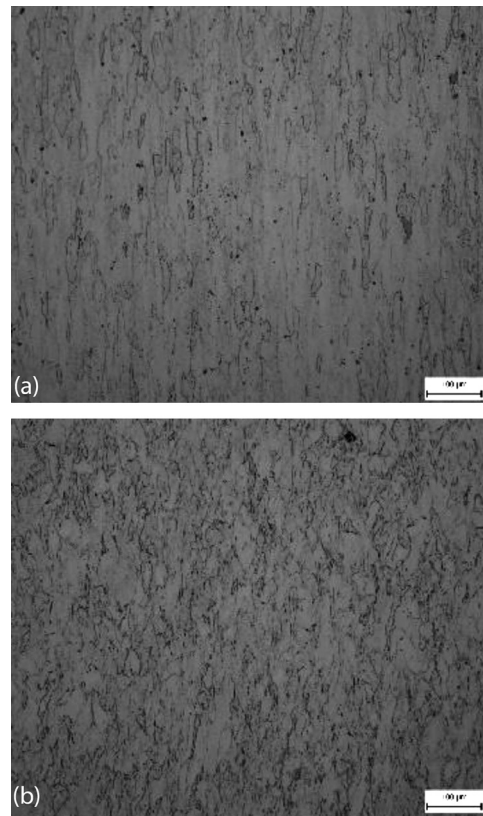


Figure 8: Microstructure for material 1 without annealing: a) without deformation, b) with 50 % deformation

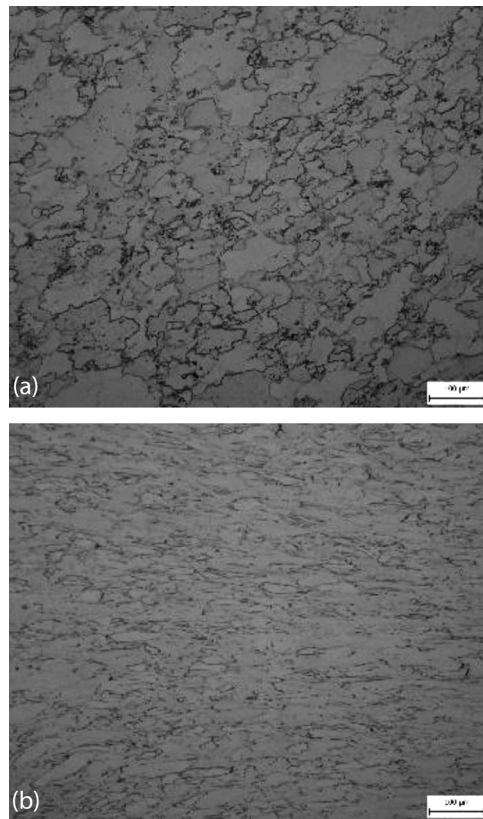


Figure 9: Microstructure of material 2 without annealing: a) without deformation, b) with 50 % deformation

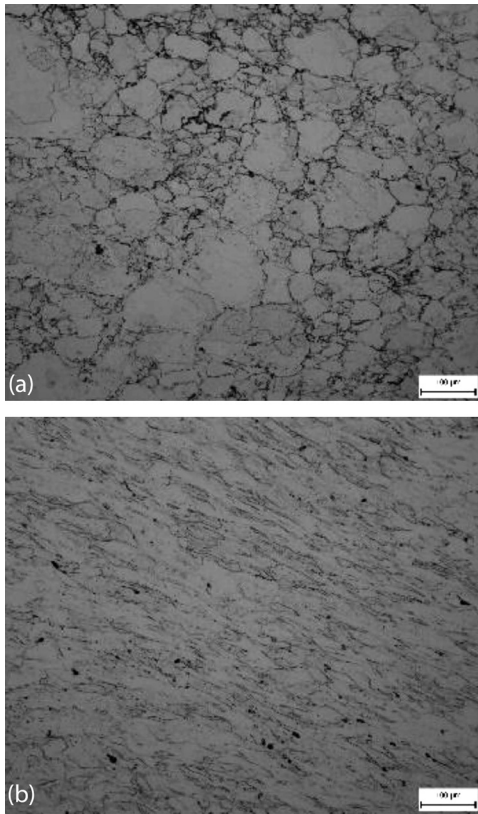


Figure 10: Microstructure for material 1 after 10 h annealing: a) without deformation, b) with 50 % deformation

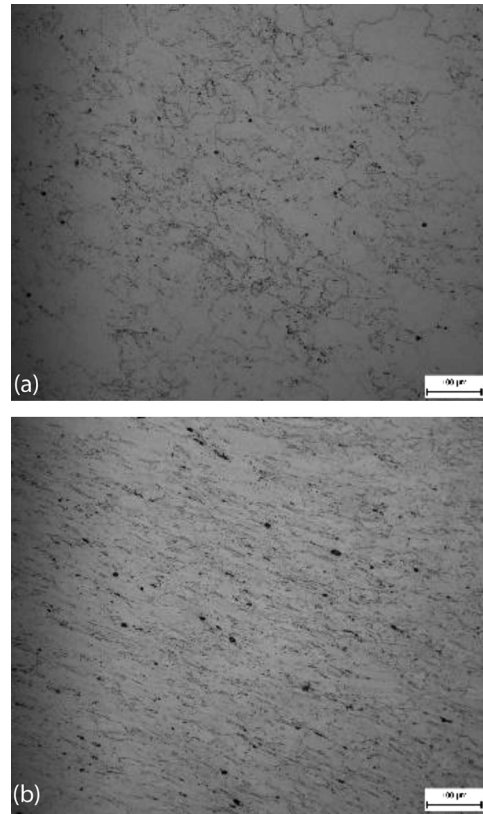


Figure 12: Microstructure for material 1 after 20 h annealing: a) without deformation, b) with 50 % deformation

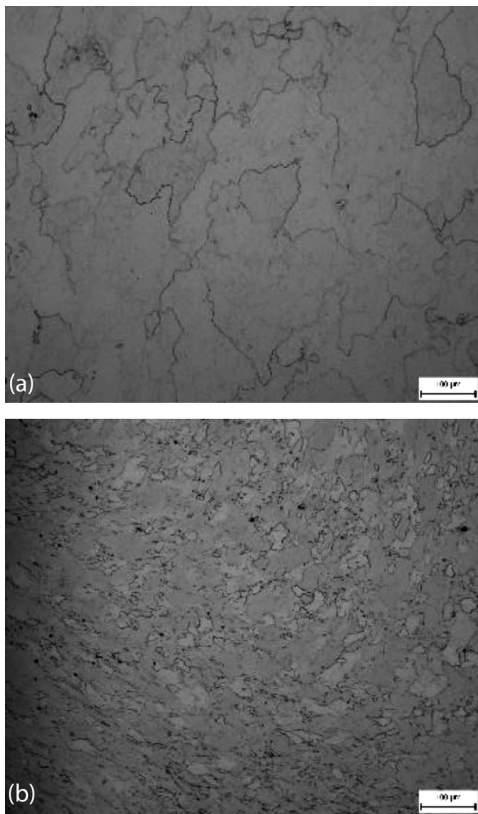


Figure 11: Microstructure for material 2 after 10 h annealing: a) without deformation, b) with 50 % deformation

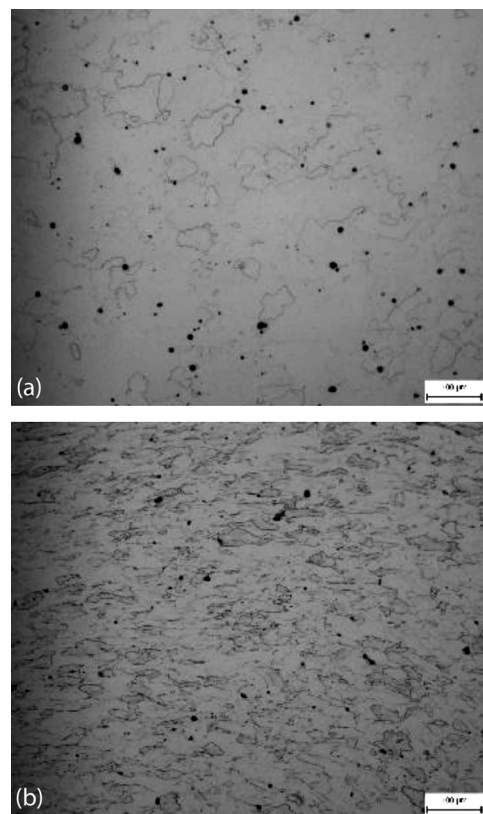


Figure 13: Microstructure for material 2 after 20 h annealing: a) without deformation, b) with 50 % deformation

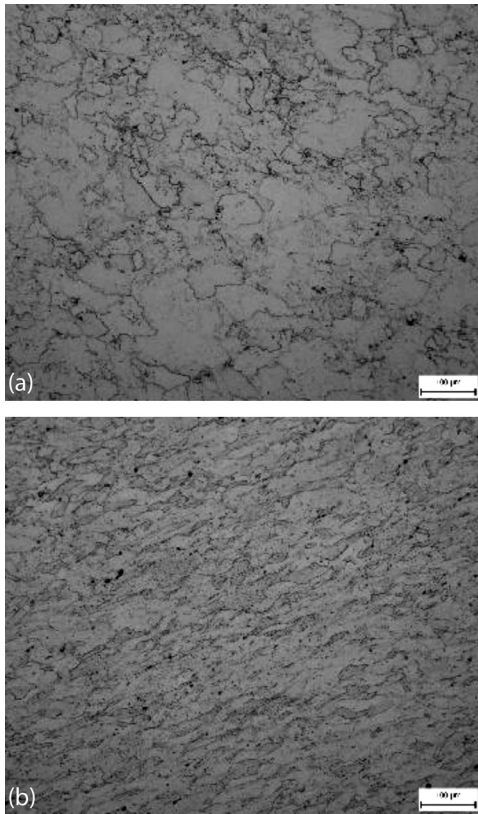


Figure 14: Microstructure for material 1 after 40 h annealing: a) without deformation, b) with 50 % deformation

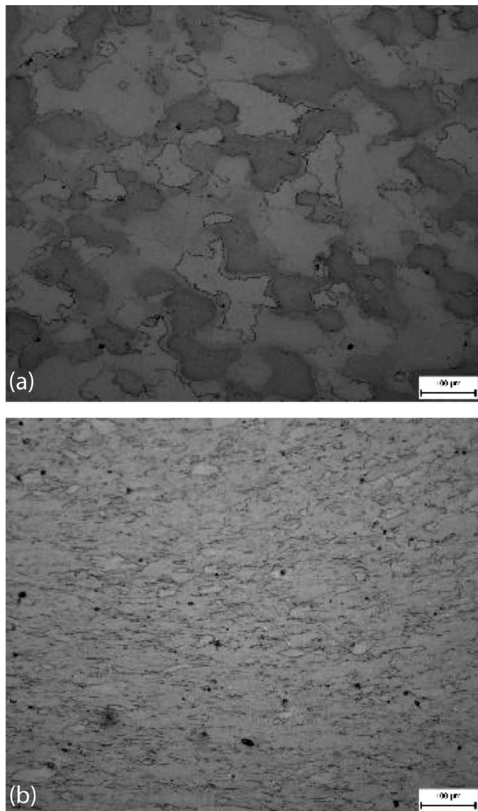


Figure 15: Microstructure for material 2 after 40 h annealing: a) without deformation, b) with 50 % deformation

sists of the Fe-Al solid solution, iron aluminide and dispersed Al_2O_3 . The grains of the solid solution are enclosed in black envelopes. The particles of Al_2O_3 are distributed throughout the structures. The influence of deformation is very obvious in the structures with the 50 % deformation. The grains are elongated and there are also subgrains.

Figure 16 gives an overview of the grain sizes for both materials with different deformations and annealing times. The grain-size measurement was done according to ASTM E112. The grain size was measured using the intersection method for the longitudinal and transverse directions. Both values were then averaged and reported as the average grain size. It can be seen that both materials are almost recrystallized with a decrease in the grain size due to the increased deformation. It is obvious that with a higher deformation applied, the grain size decreases significantly. In material 1, it decreases by almost 16 % with the change from 0 to 8 % of the applied deformation. Moreover, it decreases by almost 31 % with the change from 8 to 50 % at all the annealing times. Similarly, material 2 shows an almost 13 % decrease in the grain size with the change from 0 to 8 % and a 38 % decrease in the grain size with the change from 8 % to 50 %. On the other hand, with a constant deformation and increased holding time up to 20 h, the average grain size increases slightly. However, with the increase of the annealing time from 20 h to 40 h, it remains almost constant or decreases with some deformations. It can thus be concluded that the stability of the grain microstructure can be significantly influenced by the processing. The 20-h annealing is considered to be the optimum holding time, leading to the maximum

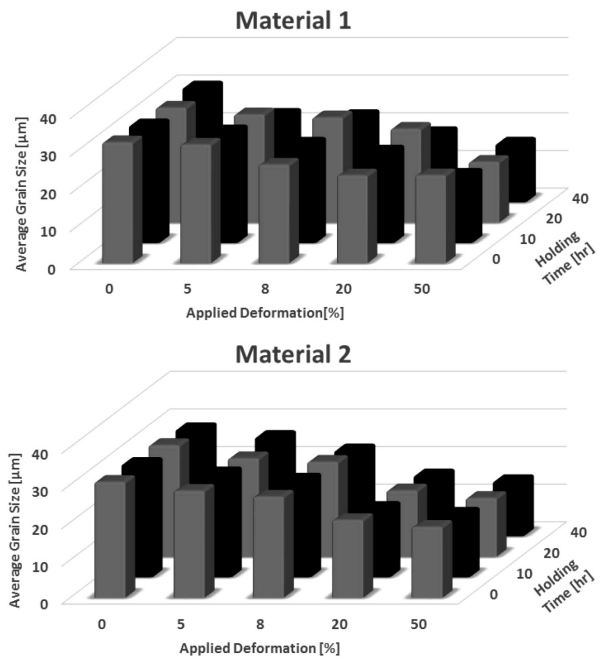


Figure 16: Average grain size for: a) material 1, b) material 2

grain growth in the ODS materials investigated in this research.

4 CONCLUSIONS

This paper outlines the influence of thermomechanical treatments on the microstructure and grain growth of new Fe-Al based alloys with fine Al₂O₃ precipitates. Two materials differing in the rolling process were tested under different conditions. The advantages of both materials are the simplicity of preparation, a low cost of the basic material and good mechanical and microstructural properties due to the Fe-Al based ferritic matrix of the ODS alloy. The results show that there is a significant reduction in the UTS with the temperature increase from RT to 800 °C; however, there is no change in the elongation. With the temperature increase from 800 °C to 1200 °C, there is no significant change in the UTS; however, the elongation decreases significantly. The holding time and applied deformation have almost no effect on the hardness of either material; however, they influence the average grain size of both materials. A higher deformation leads to a smaller grain size, while an increase in the annealing time up to 20 h leads to an increase in the average grain size of the ODS material.

Acknowledgements

This paper includes the results created within project 17-01641S Improvement of Properties and Complex Characterization of New Generation Fe-Al-O Based Oxide Precipitation Hardened Steels subsidised by the Czech Science Foundation from the specific resources of the state budget of the Czech Republic for research and development.

5 REFERENCES

- ¹ M. Mohan, R. Subramanian, Z. Alam, P. C. Angelo, Evaluation of the Mechanical Properties of a Hot Isostatically Pressed Yttria-Dispersed Nickel-Based Superalloy, *Materials and technology*, 48 (2014) 6, 899–904
- ² W. Quadackers, Oxidation of ODS alloys, *Journal de Physique IV*, 03 (1993) C9, 177–186, doi:10.1051/jp4:1993916
- ³ F. Pedraza, Low Energy-High Flux Nitridation of Metal Alloys: Mechanisms, Microstructures and High Temperature Oxidation Behaviour, *Mater. Tehnol.*, 42 (2008) 4, 157–169
- ⁴ F. Savart, Researches on the elasticity of regularly crystallized bodies, *The Edinburgh Journal of Science*, 1 (1829), 141–7
- ⁵ F. Savart, Researches on the structure of metals, as indicated by their acoustic properties, *The Edinburgh Journal of Science*, 2 (1829), 104–11
- ⁶ H. C. Sorby, On the microscopic structures of iron and study of microscopic structures of steel, *Journal of Iron and Steel Instrumentation*, 1 (1886), 140
- ⁷ F. D. Fischer, J. Svoboda, P. Fratzl, A thermodynamic approach to grain growth and coarsening, *Philosophical Magazine*, 83 (2003) 9, 1075–1093, doi:10.1080/0141861031000068966
- ⁸ O. Khalaj, B. Mašek, H. Jirkova, A. Roneseva, J. Svoboda, Investigation on New Creep and Oxidation Resistant Materials, *Mater. Tehnol.*, 49 (2015) 4, 173–179, doi:10.17222/mit.2014.210
- ⁹ M. J. Alinger, G. R. Odette, D. T. Hoelzer, On the role of alloy composition and processing parameters in nanocluster formation and dispersion strengthening in nanostructured ferritic alloys, *Acta Materialia*, 57 (2009) 2, 392–406, doi:10.1016/j.actamat.2008.09.025
- ¹⁰ P. Unifantowicz, Z. Oksiuta, P. Olier, Y. de Carlan, N. Baluc, Microstructure and mechanical properties of an ODS RAF steel fabricated by hot extrusion or hot isostatic pressing, *Fusion Engineering and Design*, 86 (2011), 2413–2416, doi:10.1016/j.fusengdes.2011.01.022
- ¹¹ M. A. Auger, V. de Castro, T. Leguey, A. Muñoz, R. Pareja, Microstructure and mechanical behavior of ODS and non-ODS Fe-14Cr model alloys produced by spark plasma sintering, *Journal of Nuclear Materials*, 436 (2013) 5, 68–75, doi:10.1016/j.jnucmat.2013.01.331
- ¹² M. Kos, J. Ferces, M. Brnucko, R. Rudolf, I. Anzel, Pressing of Partially Oxide-Dispersion-Strengthened Copper Using the ECAP Process, *Mater. Tehnol.*, 48 (2014) 3, 379–384
- ¹³ B. Mašek, O. Khalaj, Z. Nový, T. Kubina, H. Jirkova, J. Svoboda, C. Štádlér, Behaviour of New ODS Alloys under Single and Multiple Deformation, *Mater. Tehnol.*, 50 (2016) 6, 891–898, doi:10.17222/mit.2015.156
- ¹⁴ P. Marmy, T. Kruml, Low cycle fatigue of Eurofer 97, *Journal of Nuclear Materials*, 377 (2008) 1, 52–58, doi:10.1016/j.jnucmat.2008.02.054
- ¹⁵ M. Misovic, N. Tadic, M. Jacimovic, M. Janjic, Deformations and Velocities during the Cold Rolling of Aluminium Alloys, *Mater. Tehnol.*, 50 (2016) 1, 59–67, doi:10.17222/mit.2014.250
- ¹⁶ A. Grajcar, Microstructure Evolution of Advanced High-Strength Trip-Aided Bainitic Steel, *Mater. Tehnol.*, 49 (2015) 5, 715–720, doi:10.17222/mit.2014.154
- ¹⁷ B. Sustarsic, I. Paulin, M. Godec, S. Glodez, M. Sori, J. Flaker, A. Korosec, S. Kores, G. Abramovic, DSC/TG of Al-Based Alloyed Powders for P/M Applications, *Mater. Tehnol.*, 48 (2014) 4, 439–450
- ¹⁸ O. Khalaj, B. Mašek, H. Jirková, D. Bublíková, J. Svobodá, Influence of Thermomechanical Treatment on Grain Growth Behaviour of New Fe-Al Based Alloys with fine Al₂O₃ Precipitates, *Mater. Technol.*, 51 (2017) 5, 759–768, doi:10.17222/mit.2016.232
- ¹⁹ A. Kocijan, I. Paulin, C. Donik, M. Hocevar, K. Zelic, M. Godec, Influence of Different Production Progresses on the Biodegradability of AN FeMn17 Alloy, *Materials and technology*, 50 (2016) 5, 805–811, doi:10.17222/mit.2016.055
- ²⁰ D. Kumar, U. Prakash, V. V. Dabhade, K. Laha, T. Sakthivel, High yttria ferritic ODS steels through powder forging, *Journal of Nuclear Materials*, 488 (2017), 75–82, doi:10.1016/j.jnucmat.2016.12.043
- ²¹ L. Straßberger, D. Litvinov, J. Aktaa, High temperature tensile properties of oxide dispersion strengthened T91 and their correlation with microstructural evolution, *Materials Science and Technology*, 30 (2014) 13, 1691–1696, doi:10.1179/1743284714Y.0000000562
- ²² H. Dong, L. Yu, Y. Liu, Ch. Liu, H. Li, J. Wu, Enhancement of tensile properties due to microstructure optimization in ODS steels by zirconium addition, *Fusion Engineering and Design*, 125 (2017), 402–406, doi:10.1016/j.fusengdes.2017.03.170